J. Phys.: Condens. Matter 4 (1992) 7531–7544. Printed in the UK

Quantum chemical simulations of hole self-trapping in corundum

P W M Jacobs†, E A Kotomin†‡, A Stashans‡, E V Stefanovich‡ and I Tale‡

† Center for Chemical Physics, The University of Western Ontario, London, Ontario, Canada

‡ University of Latvia, 19 Rainis Boulevard, Riga, Latvia

Received 28 February 1992

Abstract. Microscopic quantum chemical calculations and simulations based on atom–atom potentials have been undertaken for hole self-trapping in pure corundum (α-Al_2O_3) crystals. A comparison of different modes of ionic relaxation during hole trapping has shown that the inward Jahn–Teller 40% displacement of two O ions accompanied by the 20% outward displacement of the two nearest Al ions is energetically the most favourable. Eighty per cent of the hole density is concentrated on these two O ions, thus confirming that a small-radius two-site polaron model, similar to that for alkali halides (the V_K centre), is applicable here. The calculated absorption energy of the STH (2.9 eV) is close to that observed experimentally.

1. Introduction

Carrier self-trapping in perfect ionic crystals, first predicted theoretically by Landau in 1933, was confirmed experimentally in 1955 by Känzig [1] who established by means of EPR that self-trapped holes (STHs) in alkali halides have the structure of X_2^- quasi-molecules (where X^- denotes a halogen ion) oriented along the ⟨110⟩ axis in FCC crystals. In recognition of his discovery they were called V_K centres. Since then STHs have been found in many ionic solids, including alkaline earth fluorides and crystals with $KMgF_3$ and PbFCl structures, as well as in rare-gas crystals [2–6]. The existence of a number of hole centres has also been established in *oxide crystals* [7], including simple alkaline earth oxides (MgO, CaO, SrO) with the cubic rock-salt structure. However, in these crystals holes (known as V^-, V^0, $[Li]^0$ centres etc.) are trapped at oxygen ions near a cation vacancy or impurity and there is no direct EPR or ENDOR evidence for their self-trapping in a *regular* oxide lattice. The only exceptions are recent EPR experiments [8] which have revealed O_2^{3-} molecular centres in *fused* silica (SiO_2); however, hole trapping in a glassy network could be assisted by charge or density fluctuations.

An experimental technique developed in the 1970s [9] may be used to detect reactions controlled by *small-polaron motion* and subsequent tunnelling recombination with electron centres by monitoring the transient kinetics of the decay of recombination luminescence in irradiated insulating solids. This method indicated the existence of small polarons in a number of materials, including AlN, $Ba_3(PO_4)_2$, the Na salt of DNA and pure α-Al_2O_3 (*corundum*) (see [10, 11] for more details). The thermally

0953-8984/92/377531+14$04.50

stimulated luminescence (TSL) peak at 220 K in crystals of the latter material were attributed to the STH motion characterized by a *hopping activation energy* of 0.7 eV and a tunnelling recombination with F centres with a photon energy of 4.3 eV.

However, this interpretation did not find universal acceptance [12]; therefore the problem of hole self-trapping in oxide crystals remains an open question. Moreover, several qualitative theoretical attempts [13, 14] undertaken in the 1970s in terms of a continuum formalism suggested the existence of *large-radius* hole polarons in corundum, in remarkable contrast with atomistic atom–atom potential calculations [15] which favoured the small single-site polaron (O^-) model!

Despite corundum's technological, mineralogical, ceramic and catalytic importance, its fusion and IR fibre applications and prospects as a laser material, electronic defects in this material have not been well studied so far [12, 16], especially theoretically. The obvious reasons for this are its quite complicated structure and the semi-covalent character of the chemical bonding [17]. The first *ab initio* periodical calculations even of a perfect corundum crystal were done only a few years ago [18–20] and these confirmed the mixed character of the chemical bonding. Despite considerable progress achieved over the last decade in the understanding of the mechanism of hole self-trapping in ionic materials [21–24], these studies are macroscopic in nature and ignore the actual electronic structure of the materials or use crude model Hamiltonians or *a priori* assumptions about the nature of the chemical bonding in the solid under investigation. This shortcoming could be overcome by means of *quantum chemical methods*. In recent years, these methods, making no *a priori* assumptions about the electronic density distribution in the perfect solid or in the vicinity of the defect under study (and often not even about the ionic relaxation in the surrounding lattice), have been used many times for the investigation of spectroscopic properties of point defects in wide-gap insulating solids [24–35] and have demonstrated their high reliability.

The main goal of this paper is to determine theoretically whether hole self-trapping can occur in corundum. With this in mind we have attempted to estimate, firstly, the energetic preference for this process, including the *relaxation energy* of a hole in pure α-Al_2O_3. The second purpose of our investigation is to determine the nature of hole localization (if any): whether it occurs on a single ion (as in AgCl), on two oxygens (like the V_K centre in alkali halide crystals) or in the three O ions which form a basic structural element in the corundum unit cell.

We present below detailed results of calculations obtained by means of the modified semi-empirical intermediate neglect of differential overlap (INDO) method [28, 29, 34, 35, 36] which has previously been applied to point defects in a number of ionic crystals, including oxides [27, 28, 34]. Due to its semi-empirical character, this method, as implemented in the CLUSTER code, allows one to construct defective clusters containing up to several tens of atoms (35 atoms in our case) and to model many possible ways of ionic relaxation, which are of primary importance in the simulation of defect processes in crystals [37]. To check our semi-empirical calculations, *ab initio* Hartree–Fock calculations were also performed for a 5-atom cluster. And lastly, the simulations based on atom–atom potentials, as implemented in the CASCADE code [38], were used to find the equilibrium geometry around the defect and the polarization energy. This technique permits the explicit automatic relaxation of several scores of the surrounding atoms (150 in our case) rather than just several atoms as in the semi-empirical calculation.

2. Semi-empirical INDO parametrization—perfect corundum

The structure of a corundum crystal may be described as hexagonal close packing of O ions with Al ions occupying two-thirds of the octahedral interstices. (Thus the Al substructure is analogous to that of rhombohedral graphite.) Each Al ion in this stucture has three nearest-neighbour O ions at a distance of 1.84 Å and three next-nearest O ions at a distance of 1.98 Å. Each O ion is surrounded by four Al ions, two at each of these distances. The unit cell of α-Al_2O_3 contains two molecular units for a total of ten atoms [39]. Good illustrations of the corundum structure are given in [12, 39]. Since chemical bonding in corundum has both ionic and covalent contributions [18], special attention has to be paid to the correct choice of the size of defect region and the interaction between this region and the rest of a crystal. The interaction of the defect region with the surrounding lattice is made most correctly in periodic models; for example, see exciton calculations in SiO_2 [34]. However, since a hole is a *charged* intrinsic defect its simulation by periodic models is not possible without the inclusion of some compensating change [40, 41]; we have therefore chosen to use the *embedded molecular cluster model* [42] with clusters large enough to incorporate the covalent nature of the chemical bonding around the self-trapped hole. The semi-empirical INDO method used allows a compromise between a large enough cluster and the accuracy of the results. Interaction of cluster ions with their surroundings was incorporated by embedding them in a rigid non-point lattice and the Coulomb interaction outside the cluster was described in the same way as inside it. The charge distribution in a crystal outside a defective cluster was obtained using the periodic large-unit-cell model [25, 26, 33] and then remained unchanged during defect calculations.

In the modified INDO calculation scheme each atom has the following parameters: Slater's orbital exponent ζ, electro-negativity E_{neg}, resonant integral parameter β, and a parameter defining populations of atomic orbitals P^0. In particular, the interaction of an electron in the orbital μ of atom A with the core of atom B, is described by

$$V_{\mu B} = Z_B \{R_{AB}^{-1} + [(\mu\mu|\nu\nu) - R_{AB}^{-1}] \exp(-\alpha_{\mu B} R_{AB})\} \qquad (1)$$

where Z_B is the charge on the core of B, R_{AB} is the distance between atoms A and B, ν is an s-orbital centred on atom B and $(\mu\mu|\nu\nu)$ is a Coulomb integral. The parameter α thus incorporates the non-point-ion character of this interaction.

To optimize the INDO parameter set, the electronic structure of a pure α-Al_2O_3 crystal was calculated using the embedded-cluster and LUC models. Al parameters were calculated through basic properties (equilibrium distance between the atoms in the molecule, and the dissociation energy) of nine Al and O related diatomic and triatomic molecules and the main features of the band structure of the perfect crystal (midpoint and width of the upper valence band, the forbidden gap, the effective charges of the ions) and the lattice constant. (Here we should mention that the calibration of parameters involves a reasonable compromise between fitting the band structure of the pure crystal and the main properties of the molecules.) The Al parameters thus obtained are shown in tables 1, 2; O parameters were taken from SiO_2 calculations [28, 34]. Table 3 presents molecular properties and table 4 gives results of electronic structure calculations for perfect corundum.

The correct symmetry and nature of the ground state for all molecules listed in table 3 are obtained. The equilibrium distances found in molecules are in good

Table 1. INDO parameter set.

Atom	AO	ζ (au)	E_{neg} (eV)	$-\beta$ (eV)	$P^0(e)$
Al	3s	1.6	17.15	1.5	0.71
	3p	1.5	12.5	1.5	0.39
O	2s	2.27	4.5	16.0	1.97
	2p	1.86	−12.6	16.0	1.96
F	2s	2.2	23.24	9.0	1.97
	2p	1.9	4.1	9.0	1.97
Cl	3s	2.1	22.35	9.0	1.98
	3p	1.76	2.7	9.0	1.97

Table 2. The electron–core interaction parameter α_{AB} (au^{-1}).

A	B			
	Al	O	F	Cl
Al	0.05	0.0	0.0	0.1
O	0.3	0.,15	—	—
F	0.45	—	—	—
Cl	0.05	—	—	—

Table 3. Properties of small Al-containing molecules. R_e is the interatomic distance (in Å), D_e the dissociation energy (in eV), q the effective charge on the atom (in e). The point group symmetry obtained for Al_2O_3 and $Al_2O_3^+$ molecules is D_{3h}.

Molecule	AlO	AlCl	AlF	AlO_2	Al_2O	Al_2O^+	Al_2	Al_2O_3	$Al_2O_3^+$
INDO									
R_e	3.0	4.0	3.1	3.2	3.2	3.1	4.4	3.2	3.1
D_e	6.5	5.4	7.0	4.4	3.7	8.6	1.7	22.4	29.5
q_{Al}	0.7	0.34	0.7	0.79	0.48	0.95			
Al–O–Al angle					145°	157°			
Experiment [45]									
R_e	3.1	4.0	3.1	3.2	3.3	3.19	4.6		
D_e	5.3	5.1	6.9	1.9	1.2	6.34	1.55		
Al–O–Al angle					144°	155°			

agreement with the experimental results. The same is true for dissociation energies, except for the molecules AlO_2, Al_2O and Al_2O^+. The behaviour of potential curves near minima is in most cases very close to the results of *ab initio* calculations.

We have used several different clusters, the sizes of which were chosen with the following principles in mind: the symmetry of a cluster has to be high enough and the cluster has to be stoichiometric [37, 44]; in constructing clusters we adhered to opinions in modern quantum chemistry about *localized groups* of electrons (or structural elements), which had been used successfully earlier [26, 37, 44]. The gist of this procedure is to construct a cluster having an integer number of structural elements (or molecular units as it is in our case for partly ionic compounds) which

Table 4. The Cartesian coordinates (in Å) of ions in the unrelaxed $[Al_8O_{12}]^0$ cluster.

Atom	x	y	z
Al(1)	0	0	4.6105
Al(2)	0	0	1.8832
Al(3)	−2.7395	0	4.0478
Al(4)	1.3697	2.3724	4.0478
Al(5)	1.3697	2.3724	4.0478
Al(6)	2.7395	0	2.4459
Al(7)	1.3697	−2.3724	2.4459
Al(8)	−1.3697	−2.3724	2.4459
O(1)	−1.2451	0.7188	3.2469
O(2)	1.2451	0.7188	3.2469
O(3)	0	−1.4377	3.2469
O(4)	2.8641	−1.6536	3.2469
O(5)	−2.8641	−1.6536	3.2469
O(6)	0	3.3072	3.2469
O(7)	0.1246	1.6536	5.4114
O(8)	1.3697	−0.9347	5.4114
O(9)	−1.4944	−0.7188	5.4114
O(10)	−0.1246	1.6536	1.0823
O(11)	−1.3697	−0.9347	1.0823
O(12)	1.4944	−0.7188	1.0823

allows one to consider more correctly the interaction between such a cluster and its environment. This is feasible due to small correlation effects between the groups of electrons mentioned above. Thus the cluster $[Al_4O_6]$ just coincides with the unit cell (two molecular units) of corundum, the cluster $[Al_8O_{12}]$ with four molecular units, and lastly the cluster $[Al_{14}O_{21}]$ consists of seven molecular units—one of them is situated in the centre of a cluster with the others placed symmetrically around it. These six molecular units form the immediate neighbourhood to the first unit. This approach enables us to consider correctly the Coulomb interaction of cluster ions with their vicinity and also the partly covalent nature of chemical bonding in corundum. The $[Al_8O_{12}]$ cluster is shown in figure 1 and Cartesian coordinates for the ions are given in table 4. This cluster is constructed around the three O ions forming the basic element of the unit cell—the oxygen triangle—and is the most compact of all the possible clusters. The compact shape of a molecular cluster reduces the effects of the cluster surface and this was indeed observed in our calculations on corundum.

In the remaining part of this section we will consider results regarding the properties of perfect corundum, which is a starting point for further defect studies. In LUC calculations, the optimized translational vectors retained unit-cell symmetry but were all 5% less than experimental values [39]. We have calculated two LUCs: Al_4O_6 which is equal to the primitive unit cell and $Al_{32}O_{48}$ which enlarges the primitive unit cell by a factor of eight. When optimizing the lattice spacing the bulk modulus $K = V\,\partial^2 E/\partial V^2$ was found to be 3.52×10^{13} dyn cm^{-2} compared with the experimental value of 3.10×10^{13} dyn cm^{-2}.

In order to diminish the effects of the cluster boundary, surface ions therein were allowed to relax; this is an additional factor which helps to describe the interaction between ions more correctly. Thus a reduction in the relative inter-ion distances for O ions by $\approx 7\%$ in the surface of the Al_4O_6 cluster and by $\approx 5\%$ in the $Al_{14}O_{21}$ cluster

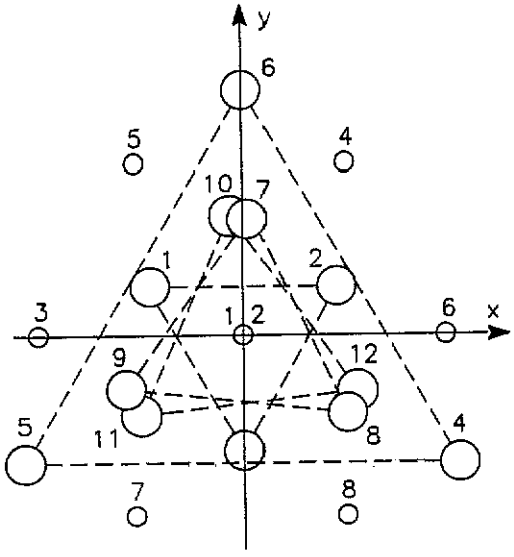

Figure 1. The projection of atoms in the $[Al_8O_{12}]$ cluster on to the x, y plane. Ions O(1), O(2), Al(1), Al(2) are used in further simulations of the hole trapping. Small circles are Al atoms, large circles, O atoms.

was observed. (These figures are given with respect to the optimized LUC geometry.) This alteration in ion positions is towards the centre of the corresponding molecular unit. Additionally, an inward displacement of Al ions ranging from 8 to 12% of the initial values was obtained and it demonstrates once more cluster-boundary effects and the covalent contribution to chemical bonding in corundum. All the following calculations of the band-structure properties were made on the *relaxed* perfect clusters and were compared with corresponding LUC results: their overall good agreement is seen from table 5. Our effective charges from Löwdin population analysis are much larger numerically than the experimental values from x-ray refinement [17], but this is also a feature of *ab initio* Hartree–Fock LCAO calculations [19] which yield $-1.37e$ for $q(0)$ from Mulliken population data for a basis set with d functions on both Al and O. The disagreement with experimental charges is mainly due to the one-exponential Slater basis set used in the INDO method, the effect of basis set expansion being well seen in Hartree–Fock calculations [18, 19]. The optical energy gap is too wide due to the omission of long-range correlation effects; only the short-range correlation correction is accounted for in INDO calculations through the use of atomic parameters which conform with [25]. Long-range correlation (between valence electrons) is known to raise the upper valence band and lower the bottom of the conduction band and that is why one has to reduce the calculated optical gap for oxide crystals by 3–5 eV. The discrepancy between the upper valence band midpoint and the experimental result [46] is not important here, because for our purpose the band width and dispersion are the most significant features. Our results with regard to the upper valence band agree quite well with *ab initio* Hartree–Fock corundum calculations (see [18, 19] and references therein). The valence band is composed of O 2p states with Al 3s (in the top of the band) and O 2s and Al 3p (in the bottom) states. The ample amount of Al in the upper valence band testifies to the considerable covalent contribution to bonding in the α-Al_2O_3 crystal. Al–O bond populations suggest essentially the same thing (in spite of the overestimated effective charges for the ions). We conclude that the above-mentioned neutral stoichiometric

clusters reproduce quite well the band structure properties and the partly covalent character of chemical bonding in corundum.

Table 5. Calculated basic band structure features of perfect corundum. ΔE_g is the optical gap, E_{vb}^{w} and E_{vb}^{m} are the width and midpoint (measured from the middle of the band gap) of the upper valence band. All energies are in eV. $q(O)$ is the effective charge on an O atom (in e).

	LUC		Neutral clusters			Expt
Feature	Al_4O_6	$Al_{32}O_{48}$	$[Al_4O_6]$	$[Al_8O_{12}]^0$	$[Al_{14}O_{21}]^0$	[17, 45]
ΔE_g [a]	12.7	11.6	13.5	12.9	12.8	9.5
E_{vb}^{w}	10.2	11.1	7.3	7.6	8.6	8.5
E_{vb}^{m}	−16.1	−16.2	−14.7	−15.4	−15.7	−20.0
$q(O)$ [c]	−1.59	−1.56	−1.73	−1.64 [b]	−1.66 [b]	−0.88

[a] Without taking into account correlation effects.

[b] Charges augment on ions situated further from the geometric centre of system; the dispersion of charges is approximately 0.1e.

[c] Löwdin's analysis yields the populations of two kinds of Al–O bonds, $q = 0.28$ ($R = 1.84$ Å), $q = 0.17$ ($R = 1.98$ Å), which are similar to Hartree–Fock values [18].

To verify the Al parameters, we have carried out additional *ab initio* Hartree–Fock LCAO pseudopotential calculations for a small $[Al_2O_3]$ cluster embedded in a point-ion crystalline field using the 2-1G Gaussian basis set [47]. This basis set consisted of 3s, 3p Al atomic orbitals (AOs) and 2s, 2p O AOs respectively. In using the pseudopotential method [48], we took recurrence formulae for the angular parts of the matrix elements of a pseudopotential [49] and calculated these matrix elements according to [50].

In comparing the results observed by semi-empirical and non-empirical methods, principal attention was paid to the symmetry analysis of the ground state of the $[Al_2O_3]$ cluster (D_{3h} symmetry group [51]). This analysis was carried out for the clusters embedded in various surrounding electrostatic fields including for *ab initio* computations: $q_{Al} = 0e$ (isolated molecule); $q_{Al} = 1.32e$ (the experimental charges [17]); $q_{Al} = 2.4e$ (the charges obtained in our LUC calculation); and lastly $q_{Al} = 3.0e$ (the fully ionic situation). Only $q_{Al} = 0e$ and $q_{Al} = 2.4e$ were used in INDO calculations. The results obtained by different methods appear to match quite well (figure 2); the ground-state symmetry is the same with insignificant differences in the one-electron energy level sequence.

The results of the electronic structure features obtained for the non-empirical $[Al_2O_3]$ cluster method are summarized in table 6. Despite the variation of charges creating the electrostatic field in which the cluster is embedded, some properties (upper valence band width and its midpoint) vary only slightly. However, the ionicity of the chemical bond depends strongly on the value of the crystalline field. Therefore we conclude that even such a single molecular unit containing five atoms is able to describe bulk band-structure properties quite reasonably (this was observed in earlier calculations [37, 44] for SiO_2 in which the chemical bonding is also partly covalent).

3. Simulation of the self-trapped hole

When a hole is inserted into the perfectly relaxed cluster, it occupies in its ground

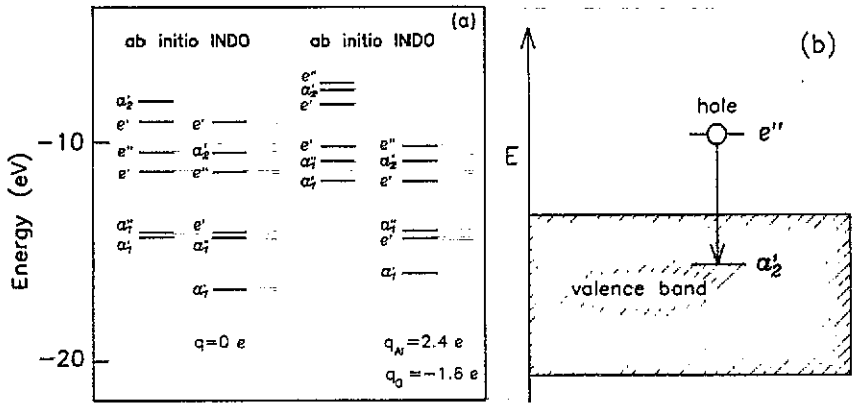

Figure 2. (*a*) One-electron energy levels for the $[Al_2O_3]^0$ cluster calculated using *ab initio* and INDO methods and embedded into lattice with two different charges on ions. (*b*) The absorption transition in the self-trapped hole.

Table 6. The dependence of band-structure features on the lattice ion charges used in non-empirical calculations on the Al_2O_3 cluster (see table 4 for notations).

Feature	Charges of lattice ions outside cluster			
	$q_{Al} = 0$	$q_{Al} = 1.32$	$q_{Al} = 2.4$	$q_{Al} = 3.0$
ΔE^w_{vb}	5.1	4.1	3.8	3.8
E^m_{vb}	−12.0	−10.2	−10.8	−11.3
q_{Al} [a] (cluster)	1.2	1.5	1.84	1.98

[a] Using Mulliken analysis to calculate effective charges on the ions, $q_O = \frac{3}{2} q_{Al}$.

state the twofold-degenerate orbital e'' (see figure 2). One therefore expects a lowering of symmetry due to the Jahn–Teller effect [52, 53] which will reduce the total energy of the system. We have simulated several relaxation modes (figure 3): (i) the displacement of a single O ion towards the centre of the basic structural O triangle, which has D_{3h} symmetry; (ii) a linear inward relaxation of two O ions; (iii) the symmetrical relaxation of all three O ions towards the centre of the triangle; and (iv) relaxation of two O ions with the bond bending expected in Jahn–Teller theory. Since e'' is an antibonding orbital for O ions and slightly bonding for the two nearest Al ions on both sides of the O triangle, we expect that an inward relaxation of O ions will be accompanied by the outward relaxation of Al ions and therefore we simulated this mode, but also considered the other relaxation modes to test our conclusions.

Results given in table 7 show the lattice relaxation obtained for various kinds of ion displacements and the relevant relaxation energies. For all three INDO clusters considered the symmetrical relaxation mode was found to be more favourable energetically than the single-atom displacement but, in its turn, less favourable than that of two O ions. Note that in all cases the hole density was shared mainly by *two* O ions, irrespective of the relaxation mode.

The role of the cation outward relaxation mode is demonstrated in figure 4 for the largest 35-atom cluster: if it were absent, O inward relaxation would result in a very flat and shallow energy minimum (≈ 0.6 eV) (curve A) whereas 20% Al relaxation

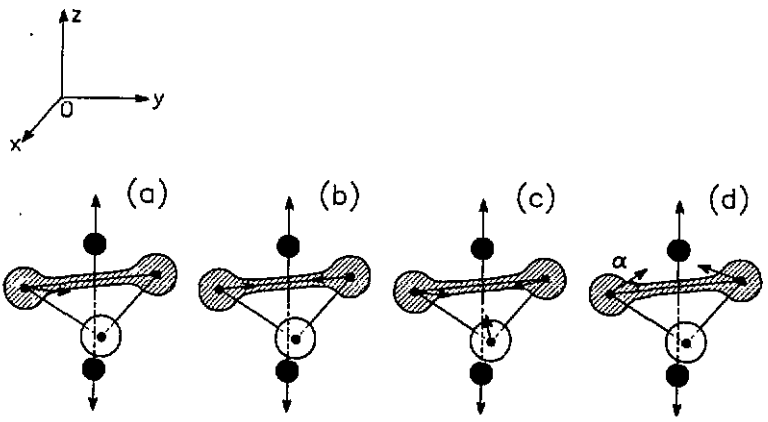

Figure 3. Different relaxation modes for simulation of hole self-trapping. (*a*) Displacement of a single O ion to the triangle centre; (*b*) symmetrical linear relaxation of two O ions; (*c*) symmetrical relaxation of three O ions; (*d*) as (*b*) but with the bond bending. Shaded dumb-bell indicates the hole density distribution.

Table 7. Calculated INDO lattice relaxation energies E_{rel} due to hole self-trapping in different clusters. Displacements of Al and O ions are given as a percentage of bond lengths, energies are in eV.

	$[Al_4O_6]^+$			$[Al_8O_{12}]^+$			$[Al_{14}O_{21}]^+$		
Cluster property	single ion	two ions	three ions	single ion	two ions	three ions	single ion	two ions	three ions
E_{rel}	1.2	3.8	2.7	1.4	3.9	2.3	1.9	5.5 [a]	4.1
ΔR_O^{in}	15	23	26	23	28	30	20	40	28
ΔR_{Al}^{outw}	16	19	19	16	19	13	16	20	23

[a] Including −0.5 eV from O–O bond bending, and −1.5 eV from Al atom relaxation.

yields a much deeper minimum of 3.5 eV in the O–O potential-energy curve (curve C). Further increase of Al relaxation makes the O–O minimum again shallower. The results of the other relaxation modes simulated are shown in figure 5, namely the O–O bond bending, which is the distinctive feature of the Jahn–Teller effect in triatomic systems [53], and the outward displacement of the third O ion in the oxygen plane. We found the last mode not to be active but bond-bending at an angle of 20° indeed reduces the total energy by an additional 0.5 eV.

The optimized geometry around the STH consists of a 40% relaxation of two O ions in the basic structural O triangle towards each other, but at an angle of 20° to the straight line joining the O sites, leaving the third O ion undisplaced, and a 20% outward displacement of the two nearest Al ions on each side of this O triangle (which contributes −1.5 eV to the total energy reduction). So the total lattice relaxation energy (with respect to the perfect cluster with an added hole) is $(-3.5 - 0.5 - 1.5)$ eV $= -5.5$ eV for the three types of displacement discussed.

Non-empirical calculations for the 5-atom cluster have confirmed qualitatively these results, but underestimate the relaxation energy by 2.5 eV; obviously this is due to the small size of this fragment. Eighty per cent of the hole density is shared by the *two* relaxed O ions reducing their effective charges from $-1.54e$ to $-1.14e$ when

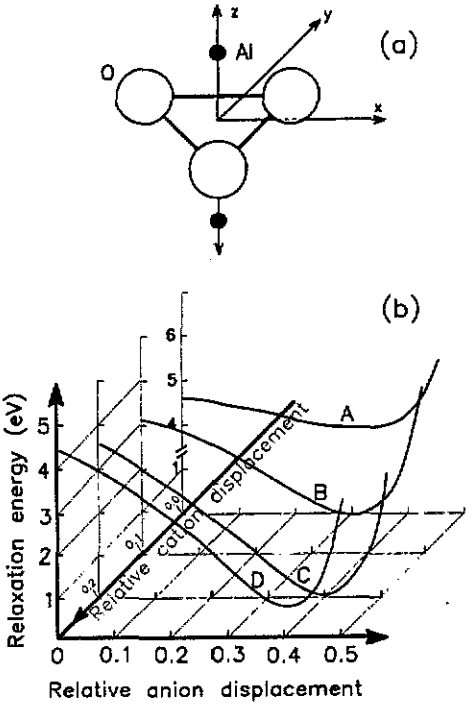

Figure 4. (*a*) Two kinds of principal ionic displacements simulating hole self-trapping: oxygen inward relaxation along the x-axis and Al outward relaxation along the z-axis. Relative relaxations are given with respect to the perfect crystal geometry, i.e. in units of the O–O distance and the Al–O plane distances respectively. (*b*) The lattice relaxation energy as a function of these two kinds of relaxations (in relative units). For the zero point the energy is taken as that of the most stable configuration (i.e. relaxations of 40% of the O–O bond and 20% of the Al–O plane distance). No bond bending is allowed.

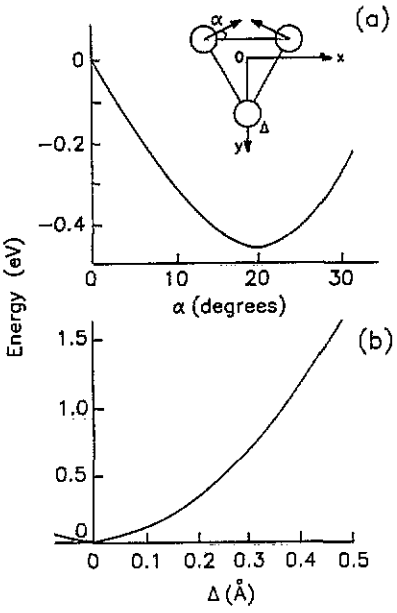

Figure 5. Optimization of the geometry of self-trapped hole with respect to the additional relaxations: (*a*) the O–O bond bending, and (*b*) displacement of the third O ion in the basic oxygen triangle.

the hole is trapped. The charge of the third O ion entering the basic structural O triangle changes insignificantly, from $-1.54e$ to $-1.48e$.

To summarize this section, we have shown the existence of a stable STH which is similar to that in alkali halides (V_K centre) and in fused silica [8] and which has the form of a considerably relaxed (with respect to perfect crystal geometry) diatomic quasi-molecule on which the hole is mainly localized; hole-trapping is associated with the essential outward relaxation of the two nearest-neighbour cations. After relaxation, the degenerate e″ hole orbital splits into two non-degenerate ones. We have calculated the absorption energy of the STH corresponding to the transition $e'' \rightarrow a_2'$ (figure 2(*b*)) of the hole (or electron transition $a_2' \rightarrow e''$), where a_2' is a one-electron wavefunction consisting of the σ $2p_x$ and $2p_y$ orbitals of the two O ions constituting the STH: its energy level lies within the valence band. The calculated absorption energy (by the ΔSCF method) is found to lie between 2.7 and 2.9 eV

(depending on cluster size) which is in quite reasonable agreement with the observed experimental value of ≈ 3.0 eV [12].

4. Cascade calculations

To check our STH geometry, we used the method of calculation based on atom–atom potentials, as implemented in the CASCADE computer code [38] for non-cubic lattices. In the last few years, this code has been used several times for defect and hole simulations in oxide crystals including the superconductor $YBaCu_3O_7$ and x-ray phosphor LaOBr [6, 54–56]. However, this code has not been used before in calculations on a relaxed STH in corundum. Previous calculations on corundum have been done by Catlow *et al* [15] who used the HADES-III computer code [15] and a *pure ionic* model for corundum (Al^{3+}, O^{2-}) with Buckingham short-range potentials of the form

$$V_{ij}(R) = A_{ij}\exp(-R/\rho_{ij}) - C_{ij}/R^6. \tag{2}$$

Since these potentials fit the cohesive energy, lattice constant, elastic constants and permittivity of corundum rather well, we also used these short-range potentials together with fully ionic charges in our CASCADE calculations. It is perhaps mildly unsatisfactory to use a fully ionic model here but it is a common feature of defect-energy calculations that this model generally works better than partially ionic models. We did make some attempts to develop a partially ionic model for corundum but failed to reproduce the basic properties of the perfect crystal, especially the cohesive energy.

In our CASCADE calculations the explicitly relaxed region I contained 150 ions. The potentials for the short-range interaction between the two O ions that share a hole are given in table 8: they were determined from the potential energy curve obtained in INDO 35-atom calculations (see figure 4(*b*)) in the same way as was done earlier for V_K centres in alkali halides [23, 57]. Short-range interactions between the O atoms constituting the STH and regular lattice ions were taken to be the same as for perfect lattice ions. (Again this is in line with V_K calculations.) Due to the strong interaction of the two O atoms sharing a hole, which is simulated by the high value for the van der Waals constant C, the potential $V(r)$ has a deep minimum of -4 eV, compared with -1 eV for the O^{2-}–O^{2-} short-range interaction; both these minima occur at practically the same separation of 1.4 Å.

With these potentials, we found an STH geometry in excellent agreement with the INDO calculations: O–O distance in the STH is reduced by 40%, the bond is bent with respect to the straight line connecting sites by an angle of 15°; two nearest Al ions are displaced outward by 25%; and third O atom in the basic triangle is practically undisplaced. Using the CASCADE code, we calculated also the electronic and ionic polarization energies which are 4.27 eV and 0.10 eV respectively. Such a great difference comes from the fact that the main contribution to the ionic polarization has already been included in the lattice relaxation energy; for example the 1.5 eV relaxation energy due to two Al ion outward displacements.

Table 8. Potential parameters for α-Al_2O_3 and the STH.

Interaction	A (eV)	ρ (Å)	C (eV Å^{-6})	Comment
O^{2-}–O^{2-} O^{2-}–O^{1-}	22764.3	0.149	22.879	a
O^{1-}–O^{1-}	52852.9	0.156	80.065	b
Shell model	K (eV Å^{-2})	Y ($\|e\|$)	Z ($\|e\|$)	
O^{2-}	103.07	−2.8106	−2.0	a
O^{1-}	103.07	−1.95061	−1.14	c
Al^{3+}	102.488	1.3830	+3.0	a

a From Catlow *et al* [15].
b By fitting INDO results for 35-atom cluster to the Buckingham potential.
c Z from INDO calculations.

5. Discussion and conclusions

The energy of self-trapping, E_{ST}, consists of four terms [58, 59]. These are the energy change as a free hole becomes localized on a single anion (E_{loc}); the loss in the polarization energy associated with the mobile hole ($-E_{pol}^{(1)}$); the energy change (E_{rlx}) associated with the five-atom cluster within which the hole is localized (namely, the basic O triangle and its two nearest-neighbour Al atoms) as they relax from perfect lattice sites; and the polarization energy $E_{pol}^{(2)}$ associated with the rest of the lattice outside the five-atom cluster

$$E_{ST} = E_{loc} - E_{pol}^{(1)} + E_{rlx} + E_{pol}^{(2)}. \tag{3}$$

Note that the reference state in calculating these terms is that of a hole localized on one O lattice site in an otherwise perfect crystal and that while $E_{pol}^{(1)}$ involves only electronic polarization (displaced shells), $E_{pol}^{(2)}$ includes both ionic and electronic polarization terms.

E_{loc} may be estimated [60] as $\simeq 75\%$ of half the width of the oxygen 2p valence band, and so ≈ 3.4 eV. The term $-E_{pol}^{(1)}$ is the difference between initial and final defect energies in a CASCADE calculation with fixed cores when the defect is a hole on one lattice site, namely 3.7 eV. The lattice E_{rlx} relaxation energy for the largest 35-atom cluster we considered was found to be −5.5 eV (which by a factor of two exceeds the value for the V_K centre in KCl). The polarization energy $E_{pol}^{(2)}$ is found as the difference between final and initial defect energies (−4.3 eV) in a CASCADE calculation in which both cores and shells relax when the defect is the five-atom cluster with the five atoms in their final positions given by the INDO calculation. The energy of the STH relative to the delocalized hole is, therefore:

$$E_{ST} = (3.4 + 3.7 - 5.5 - 4.3)\ \text{eV} = -2.7\ \text{eV}.$$

Since E_{ST} is negative, self-trapping is favoured with respect to a free delocalized hole in the valence band.

Therefore the embedded-molecular-cluster quantum chemical simulations of the STH in corundum presented here give strong support to the existence of an STH in

the form of a O_2^{2-} quasi-molecule (small-radius polaron). Additional support for this model comes from the simulation of STH *migration* [61]; the calculated activation energy by INDO for hopping ≈ 0.9 eV is in good agreement with the experimental value of 0.7 eV. Another important STH feature to be checked theoretically is the photon energy for their tunnelling recombination with F centres [10, 11]. Alternatively, greater confidence in this theory could be achieved through *ab initio* calculations on larger clusters, e.g. by means of the ICECAP code used in recent years for quite similar computer simulations [2], as well as by more accurate estimates of the hole localization energy in partly covalent solids [60, 62]. *Direct* experimental evidence for STH could be obtained only from magnetic resonance experiments and we hope this study may stimulate such a search.

Acknowledgments

Thanks are due to J Gale, E Heifets, M F Islam, V Puchin, A Shluger and J Valbis for discussions of the problems treated in this paper. EK thanks also the Centre for Chemical Physics at The University of Western Ontario for a Fellowship during the tenure of which this work was undertaken. PWMJ acknowledges partial support of this project by the Natural Sciences and Engineering Research Council of Canada.

References

[1] Känzig W 1955 *Phys. Rev.* **99** 1890
[2] Vail J M 1990 *J. Phys. Chem. Solids* **51** 589
[3] Kabler M N 1972 *Point Defects in Solids* (New York: Plenum) p 327
[4] Schoemaker D 1973 *Phys. Rev.* B **7** 786
[5] Schoemaker D and Waldner F 1971 *Helv. Phys. Acta* **44** 560
[6] Islam M 1991 *Phil. Mag.* A **64** 1119
[7] Spaeth J-M and Kroschick F K 1991 *J. Phys. Chem. Solids* **52** 1
[8] Griscom D L 1989 *Phys. Rev.* B **40** 4224
[9] Tale I and Gailitis A 1971 *Bull. Sov. Acad. Sci.* **35** 1336
[10] Kotomin E, Tale I, Tale V, Butlers P and Kulis P 1989 *J. Phys.: Condens. Matter* **1** 6777
[11] Kulis P, Rachko Z, Springis M, Tale I and Janson J 1991 *Radiat. Eff. Defects Solids* **119–121** 963
[12] Valbis J and Itoh N 1991 *Rad. Eff. Defects Solids* **116** 171
[13] Cox R T 1981 *Recent Devel. Condens. Matter Phys.* **3** 355
[14] Colbourn E A and Mackrodt W C 1981 *Solid State Commun.* **40** 265
[15] Catlow C R A, James R, Mackrodt W C and Stewart R F 1982 *Phys. Rev.* B **25** 1006
[16] Crawford J H Jr 1983 *Semicond. Insul.* **5** 599; 1984 *Nucl. Instrum. Methods* B **1** 159; 1983 *Structure of Properties of MgO and Al_2O_3 Ceramics (Advances in Ceramics 10)* ed W P Kingery (Columbus, OH: American Ceramics Society)
[17] Bialas H and Stolz H J 1975 *Z. Phys.* B **21** 319
Lewis J, Schwarzenbach D and Flack H D 1982 *Acta Crystallogr.* A **38** 733
[18] Causà M, Dovesi R, Roetti C, Kotomin A and Saunders V 1987 *Chem. Phys. Lett.* **140** 120
[19] Salasco L, Dovesi R, Orlando R, Causà M and Saunders V 1991 *Mol. Phys.* **72** 267
[20] Xu Y-N and Ching W Y 1991 *Phys. Rev.* B **43** 4461
[21] Toyozawa Y 1990 *Atomic Processes Induced by Electronic Excitations in Non-Metallic Solids* (Singapore: World Scientific) p 3
[22] Iida T and Monnier R 1976 *Phys. Status Solidi* b **74** 91
Higashimura T, Hakaoka Y and Iida T 1984 *J. Phys. C: Solid State Phys.* **17** 4127
[23] Cade P E, Stoneham A M and Tasker P W 1984 *Phys. Rev.* B **30** 4621; 1986 *Phys. Rev.* B **33** 4166
[24] Stoneham A M 1975 *Theory of Defects in Solids* (Clarendon: Oxford University Press) ch 18
[25] Evarestov R A, Kotomin E A and Ermoshkin A N 1983 *Molecular Models of Point Defects in Wide-Gap Solids* (Riga: Zinatne)

[26] Zakis Y, Kantorovich L, Kotomin E, Kuzovkov V, Tale I and Shluger A 1991 *Models of Processes in Wide-Gap Solids with Defects* (Riga: Zinatne)
[27] Shluger A L, Kotomin E A and Kantorovich L N 1986 *J. Phys. C: Solid State Phys.* **19** 4183
[28] Stefanovich E, Shidlovskaya E, Shluger A L and Zakharov M 1990 *Phys. Status Solidi* b **160** 529
[29] Shluger A L and Kotomin E A 1981 *Phys. Status Solidi* b **108** 673
[30] Rao R S, McEachern R J and Weil J A 1991 *J. Comput. Chem.* **12** 254
[31] Meng J, Jena P and Vail J M 1990 *J. Phys.: Condens. Matter* **2** 10371
[32] Mombourquette M J, Weil J A and Merey P G 1984 *Can. J. Phys.* **62** 21
[33] Evarestov R A and Lovchikov V A 1977 *Phys. Status Solidi* b **79** 743; 1979 *Phys. Status Solidi* b **93** 469
Evarestov R A, Sokolov A R, Leko A V and Verjazov V A 1989 *J. Phys.: Condens. Matter* **1** 6611
[34] Shluger A L and Stefanovich E V 1990 *Phys. Rev.* B **42** 9664
Shluger A L, Itoh N and Noda K 1991 *J. Phys.: Condens. Matter* **3** 9895
[35] Shluger A L and Itoh N 1990 *J. Phys.: Condens. Matter* **2** 4119
[36] Gavartin Y, Shidlovskaya E, Shluger A L and Varaksin A 1991 *J. Phys.: Condens. Matter* **3** 2237
[37] Kotomin E A and Shluger A L *1989 Radiat. Effects Defects Solids* **111–112** 177
[38] Leslie M 1983 *Solid State Ionics* **8** 243; 1985 *Physica* B **131** 145
[39] Wyckoff R W 1964 *Crystal Structures* (New York: Wiley)
[40] Gillan M J, Harding J and Leslie M 1988 *J. Phys. C: Solid State Phys.* **21** 5465
[41] Bar-Yam Y and Jonnopoulos J D 1984 *Phys. Rev.* B **30** 1844
[42] Kantorovich L N 1988 *J. Phys. C: Solid State Phys.* **29** 5041
[43] Evarestov R A and Smirnov V P 1987 *The Methods of Group Theory in Quantum Chemistry of Solids* (Leningrad: State University Press) (in Russian)
[44] Geisser C and Shluger A 1986 *Phys. Status Solidi* b **135** 669
[45] Krasnov K S 1979 *Molecular Constants of Non-Organic Compounds* (Leningrad: Khimiya) (in Russian)
[46] Arakawa E T, Williams M W 1968 *J. Phys. Chem. Solids* **29** 735
Balzarotti A and Bianconi A 1976 *Phys. Status Solidi* b **76** 2 689
[47] Barthelat J C, Durand P H and Serafini A 1977 *Mol. Phys.* **33** 159
[48] Bachelet G B, Hamann D R and Shlüter M 1982 *Phys. Rev.* B **26** 4199
[49] Zapol B 1986 *Proc. Lavt. Acad. Sci. Phys.* **4** 3; 1986 *Proc. Lavt. Acad. Sci. Phys.* **5** 111
[50] Zapol B P, Puchin V E, Heifets E N and Zaks I O 1989 *Sov. J. Struct. Chem.* **30** 135
[51] Elliott J P and Dawber P G 1979 *Symmetry in Physics* (London: MacMillan)
[52] Englman R 1972 *Jahn-Teller Effect in Molecules and Crystals* (New York: Wiley)
[53] Bersuker I B and Polinger V Z 1983 *Vibronic Interactions in Crystals and Molecules* (Moscow: Nauka) in Russian
[54] Jacobs P W M and Vernon M L 1990 *J. Chem. Soc. Faraday Trans.* **86** 1233
[55] Islam M S and Baetzold R C 1989 *Phys. Rev.* B **40** 10926
[56] Islam M S 1990 *Supercond. Sci. Technol.* **3** 531
[57] Monnier R, Song K S and Stoneham A M 1977 *J. Phys. C: Solid State Phys.* **10** 4441
[58] Fowler W B 1968 *Physics of Colour Centres* (New York: Academic) ch 2
[59] Gilbert T L 1966 *Lecture Notes for the NATO Summer School (Ghent)*
[60] Shluger A L, Heifets E N, Gale J D and Catlow C R A 1992 *J. Phys.: Condens. Matter* **4** 5711
[61] Jacobs P W M and Kotomin E A 1992 *Phil. Mag.* at press
[62] Shluger A L, Grimes R W, Catlow C R A and Itoh N 1991 *J. Phys.: Condens. Matter* **3** 8027
Shluger A L, Kantorovich L N, Heifets E N and Shidlovskaya E 1992 *J. Phys.: Condens. Matter* **4** 7417